

Orthogonal arrays-based method for the probabilistic voltage stability analysis of unbalanced power systems

Original

Orthogonal arrays-based method for the probabilistic voltage stability analysis of unbalanced power systems / Carpinelli, G., Russo, A., Varilone, P., Verde, P.. - In: INTERNATIONAL JOURNAL OF ELECTRICAL POWER & ENERGY SYSTEMS. - ISSN 0142-0615. - 174:(2026). [10.1016/j.ijepes.2025.111501]

Availability:

This version is available at: 11583/3009214 since: 2026-03-25T12:10:56Z

Publisher:

Elsevier Ltd

Published

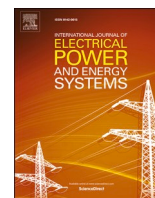
DOI:10.1016/j.ijepes.2025.111501

Terms of use:

This article is made available under terms and conditions as specified in the corresponding bibliographic description in the repository

Publisher copyright

(Article begins on next page)



Orthogonal arrays-based method for the probabilistic voltage stability analysis of unbalanced power systems

Guido Carpinelli^a, Angela Russo^{b,*}, Pietro Varilone^c, Paola Verde^c

^a Former Professor of Power System Analysis, Napoli, Italy

^b Dipartimento Energia "Galileo Ferraris", Politecnico di Torino, Italy

^c DIEL, Università di Cassino e del Lazio Meridionale, Italy

ARTICLE INFO

Keywords:

Voltage stability
Probabilistic approaches
Orthogonal arrays
Optimization methods

ABSTRACT

In the newly liberalized market, transmission and distribution systems are widely recognized as large-scale uncertain systems due to the stochastic nature of renewable generation and load demands. In this context, probabilistic voltage stability analysis is crucial for ensuring secure system operation. This paper proposes a novel probabilistic approach, the Orthogonal Arrays-Based Method (OABM), to address uncertainties in probabilistic voltage stability analysis for unbalanced power systems. OABM is a computationally efficient probabilistic approximation method that preserves the essential statistical properties of input random variables. The maximum load margin is used as the voltage stability index, and a nonlinear, constrained optimization model, employing complementarity constraints (CCs), is utilized to identify critical voltage stability conditions. CCs accurately model synchronous machines, enabling a seamless transition between PV and PQ bus operation. Numerical applications on a test system, compared with more traditional probabilistic techniques such as Monte Carlo and Point Estimate methods, demonstrate the high accuracy and low computational cost of the proposed OABM approach.

1. Introduction

1.1. Background and motivation

Increased renewable energy and load demands make Voltage Stability (VS) a key concern for power grid operators. VS is the power system's ability to maintain steady voltage levels after small or large disturbances. Instability leads to progressive voltage changes.

The small-disturbance (static) VS can be analyzed through steady-state analyses as well as linearization of the system modelling [1,2]. Continuation power flow (CPF), modal decomposition (MD), and optimization methods (OMs) have been usefully applied [2–5]. The CPF starts with an initial operating condition and goes on through a predictor–corrector scheme to find the VS limit condition. MD elaborates the eigensystem of the reduced Jacobian matrix and provides information about the proximity to instability. OMs determine the limit condition, typically the maximum load margin, which quantifies how far the current operating point is from the VS critical point. Its maximum value is consistently used to characterize VS due to its ease of understanding and use for operators [6], and it is usually obtained by solving a non-

linear, constrained optimization problem. CPF and OMs are the tools most frequently used.

Regardless of the method employed, traditional voltage stability analysis often relies on balanced system assumptions, even though unbalanced conditions can lead to significantly different stability behaviors [7,8].

Also, the significant uncertainties associated with renewable energy sources like photovoltaic and wind power, as well as load variations, have a notable impact on voltage stability conditions. Then, probabilistic voltage stability analysis (PVSA) is now widely recognized as an essential tool for power system operation and planning.

When a probabilistic perspective is adopted for voltage stability analysis (VSA), input variables like load and renewable generation powers are treated as random variables (RVs) with associated probability density functions (PDFs). These PDFs can be assumed to follow known distributions (e.g., normal, Weibull, Beta) or can be estimated from historical data. The dependencies among input variables, both spatial and temporal, should be accurately modeled.

Once the statistical characteristics of the input variables are defined, the goal is to determine the probabilistic characteristics of the output

* Corresponding author.

E-mail address: angela.russo@polito.it (A. Russo).

<https://doi.org/10.1016/j.ijepes.2025.111501>

Received 21 May 2025; Received in revised form 23 October 2025; Accepted 14 December 2025

Available online 6 January 2026

0142-0615/© 2025 The Author(s). Published by Elsevier Ltd. This is an open access article under the CC BY license (<http://creativecommons.org/licenses/by/4.0/>).

variables, such as the maximum load margin. Various probabilistic techniques, including Monte Carlo simulation, fuzzy methods, cumulant methods, clustering-based approaches, and robust optimization, can be employed, each with its own advantages and limitations [9].

1.2. Relevant literature

The influence of uncertainties in input variables on voltage stability phenomena makes PVSA indispensable. As a result, recent literature shows a growing interest in this area [10–31].

In [10] the Point Estimate Method is applied together with the CPF. Balanced systems are considered, and the Cornish-Fisher expansion is applied to obtain the probability distributions (PDs) of the output random variables. In [11] a probabilistic optimal power flow is formulated to maximize the load margin in an unbalanced distribution system. A modified cumulant method is applied to deal with correlations between input random variables. Cornish-Fisher and Gram-Charlier expansions are employed to obtain the PDs of the output random variables. In [12] a probabilistic multistage optimization problem is formulated for unbalanced power systems, based on the use of complementarity constraints. A traditional Monte Carlo simulation approach is applied. In [13] a risk-based PVSA is provided based on Conditional Value-at-Risk and Quasi Monte Carlo simulation. CPF is applied to balanced power systems. In [14] a probabilistic optimization model of balanced systems with high penetration of correlated renewable energy sources is first presented and then a global sensitivity analysis model is proposed to identify the most critical variables affecting the PVSA. The stochastic surrogate surface method using the polynomial chaos expansion is applied. In [15] a probabilistic index is proposed for the PVSA in distribution systems with wind energy sources. The cumulants method with the maximum entropy method is applied as probabilistic technique. The same authors in [16] use a catastrophe theory-based model to find the bifurcation point of the system. The Point Estimate Method and Cornish-Fisher series are applied to obtain the moments and the PDs of the voltages and the risk of voltage collapse. In [17] a probabilistic optimization model is formulated considering uncertainties in both loads and generations growth directions. Latin Hypercube Sampling and CPF are applied. In [18] the effect of uncertain parameters on load margin is analyzed considering uncertainties of renewable generation and loads in balanced power systems. The Morris screening sensitivity analysis method coupled with a multivariate Gaussian copula to account for parameter correlations is used for the priority ranking of uncertain parameters. In [19] the power method transformation combined with Latin hypercube sampling and a twice permutation technique is proposed for a PVSA in balanced power systems. A probabilistic optimization model able to consider different directions of generation and loads is provided. In [20] a cumulant-based maximum entropy method combined with Natan transform is applied to evidence the effects of correlated variables on maximum load margin. CPF is applied to find critical conditions. In [21] the PVSA of a balanced power system with high integration of photovoltaic systems is considered. A traditional Monte Carlo simulation approach is applied to characterize some VS indices (critical eigenvalue, reactive power margin, loading margin and real and reactive power loss). In [22] four clustering algorithms are applied to find the aggregated wind farm model characterized by the highest probability of occurrence. Then, the maximum load margin is obtained performing PV-curve calculations in DIGSILENT by simply increasing the loads. In [23] the influence of line switching on the load margin maximum values in balanced power systems is analyzed considering loads and renewable powers uncertainties. Latin hypercube sampling and copula functions are applied to generate the scenarios. Then, a scenario reduction technique, customized for the PVSA problem in study, is provided to reduce computational efforts. The CPF is applied. In [24], the optimization problem regarding the number of operations, including line switching and busbar splitting, is considered and a day-ahead voltage-stability-constrained network topology optimization

problem is formulated. CPF is applied and a process of reduction of scenarios is used. [25] considers the integrated transmission and distribution networks and the static voltage stability margin interval is determined by accounting for the uncertain of renewables; a distributed bilevel optimal power flow calculation method based on the alternating direction method of multipliers is applied. The upper and lower bounds of the stability margin interval are calculated. In [26], a probabilistic optimal power flow is formulated for balanced power systems with correlated input random variables. A variance-based Global Sensitivity Analysis approach is proposed to analyze the influence of random input. Univocal sensitivity indices are also introduced, and two efficient strategies are proposed to limit computational efforts. The Monte Carlo simulation approach is applied. In [27], the uncertain system parameters are modelled including their correlations and several alternative sampling generation techniques are employed and compared; the results demonstrate that the independent sampling technique is not adequate to represent the uncertain variables of real-world system data.

In recent years, studies applying data analysis and machine learning techniques [28–31] have been proposed following the availability of large dataset of measurements, including nodal voltage phasor data collected by PMUs. The advantage of these studies is that they can intrinsically account for uncertainty of input variables through the data itself. The objective of [28] is to estimate the prediction intervals for VS margin and, to this aim, a Box-Cox transformation method is applied to transform the available data into approximate Gaussian distributions and, then, the extreme learning machine model is set for the estimation of the target VS index. The model is updated as new data are available. [29] formulates the estimation of the probabilistic VS margin as a quantile regression problem and applies an improved deep quantile regression to determine a set of quantiles; a dynamic deep ensemble learning scheme is, then, applied to improve the performance of predictive quantiles for the VS index. In [30], based on measured data without information about the system model, a real-time matrix factorization, that separates the deterministic components and random ones (i.e., random elements caused by renewable energy sources), is proposed and the probabilistic VS index is based on the eigenvalue distribution of the random part. Finally, [31] aims to the probabilistic VS assessment of distribution systems; in particular, a single extreme learning machine (i.e., a single hidden layer feedforward neural network), able to map the relationship between input variables and VS index, is applied for the estimation of the pdf of the desired index. It is worth noting that the mentioned papers proposed methods adequate also to online estimation of voltage stability margins.

1.3. Contributions

Probabilistic voltage stability analysis in unbalanced three-phase power systems can involve a significant computational burden. This is because these systems necessitate detailed three-phase modeling of all components, including generators, transformers, lines, and loads, resulting in large-scale system representations. To address this complex challenge, this paper proposes the application of an Orthogonal Arrays-based Method (OABM). The Orthogonal Arrays (OAs) [32,33], widely adopted across various engineering disciplines [34–42], offer a significant advantage by substantially reducing the number of simulations (scenarios) required compared to traditional Monte Carlo simulations, while still maintaining the accuracy of the results. This is achieved by characterizing the input random variables with a limited set of discrete samples, rather than relying on their full probability density functions. OAs of different strengths are employed to efficiently explore the random input space as higher-strength OAs enable the modeling of more complex interactions between input random variables and are expected to yield more accurate and reliable results [32].

For each simulation, a nonlinear, constrained optimization problem is solved; the same model is applied in [43] and solved by another probabilistic approach. The model includes complementarity

constraints to identify critical voltage stability conditions, such as the maximum load margin and phase voltages. The complementarity constraints accurately represent conventional generators, enabling a seamless transition between PV and PQ bus operation as reactive power limits are reached. Even if complementarity constraints have been previously used in PVSA [12], their application was limited to a Monte Carlo-based multi-stage procedure, lacking the efficiency benefits of an OAs-based approach.

In summary, the main contributions of this paper are:

- 1) An OAs-based method is proposed to reduce computational complexity while preserving accuracy. OAs are never applied to PVSA.
- 2) OAs of different strengths are employed, a further novelty in applying OAs to PVSA.
- 3) A nonlinear, constrained optimization model, incorporating complementarity constraints, is solved to accurately determine critical voltage stability conditions. Complementarity constraints are hardly ever applied to PVSA and never in conjunction with OAs.

Numerical applications on a test system are presented to demonstrate the impact of input uncertainties and correlations on voltage stability limit conditions. Comparisons with traditional probabilistic techniques, such as Monte Carlo simulation (MCS) and Point Estimate Method, are conducted. The accuracy of our proposed approach is assessed by comparing the means, standard deviations, and probability distributions of the output random variables.

The paper is organized as follows. Section 2 presents the applied method and procedures. Section 3 describes the benchmarks methods chosen for the validation of the proposed method. Numerical applications and discussions are presented in Section 4. The conclusions are drawn in Section 5.

2. Methods and procedures

Consider a three-phase unbalanced power system with uncertainties and correlations in both renewable and load powers. Any OABM applied to the PVSA of this system involves the following steps:

1. *Identify Input Random Variables*: The input random variables (called “factors”) relevant to the voltage stability analysis, such as load and renewable generation powers, are selected.
2. *Determine Samples Number and Values for Input Random Variables*: Each factor is assigned a specific number and values of samples (called “levels”), representing different scenarios for that factor.
3. *Select Orthogonal Array*: An OA is used to efficiently select a subset of all possible factors levels combinations, optimizing the number of simulations required.
4. *Run Deterministic VSA Simulations*: For each combination of factors levels specified by the OA, a deterministic VSA simulation is performed solving a nonlinear, constrained optimization model to obtain a sample of the output variables of interest.
5. *Process Output Data*: The output results are analyzed to characterize the statistical features of the VSA output random variables, such as voltage magnitudes, voltage angles, and load margin.

By performing these steps, the OABM significantly reduces the computational burden associated with traditional Monte Carlo simulations while preserving the statistical accuracy of the results.

In the following sub-sections, firstly the details of each step are provided (Sub-sections 2.1 – 2.5), then the deterministic underlying optimization model for VSA (Sub-section 2.6) is shown.

2.1. Identify input random variables

The input random variables for the PVSA considered in this paper are load and renewable generation powers. In the OABM framework, each input random variable is referred to as a “factor” and is represented using a limited number of discrete samples, rather than its full PDF.

In the following, the terms ‘factor’ and ‘input random variable’ will be used interchangeably.

2.2. Determine samples number and values for each input random variables

The selection of the number and values of samples for each input random variable is crucial for the OABM’s effectiveness in PVSA.

The number of samples for each input variable must be carefully selected to balance accuracy and computational efficiency. While two levels (or representative points) might suffice for symmetrical variables with a predominantly linear effect, more levels (e.g., three) can be necessary for variables with asymmetric or heavy-tailed PDFs or those with a significant non-linear impact on the output [36,38,39]. Testing higher levels (e.g., 4 or 5) is rarely implemented because the resulting significant increase in computational cost typically far outweighs the marginal gain in accuracy for analysing power system uncertainties. Traditionally, the same number of levels (e.g., three) is used for all input variables.

In power system applications, the selection of samples values is typically based on the mean (μ) and standard deviation (σ) of the input random variables. For instance, two samples can be selected as $\mu - \sigma$ and $\mu + \sigma$ while three samples can be selected as $\mu - \sqrt{3/2}\sigma$, μ and $\mu + \sqrt{3/2}\sigma$. Sometimes, this approach can lead to negative values for variables with non-negative support, especially for skewed or heavy-tailed distributions. To address this problem, [44] proposed using equally spaced quantiles of the PDF. This ensures that the selected values are representative of the entire range of the distribution, even for non-symmetric distributions.

2.3. Select orthogonal array

Once the input random variables and their samples number and values are defined, a comprehensive exploration of the entire design space would require simulating the underlying VSA optimization model (see Section 2.6) for all possible combinations of input random variables values. However, this exhaustive approach is computationally cumbersome, even for moderately sized problems. For instance, in case of N_{IRV} input random variables and of N_L samples assigned to each of them, an exhaustive exploration of all possible combinations would require to run $N_{full.sim} = (N_L)^{N_{IRV}}$ simulations, which would be quite expensive computationally. For example, with three samples for each of ten input random variables, it results: $N_{full.sim} = 59049$.

OAs can be used to significantly reduce the number of deterministic VSA simulations required, from the previous full factorial number of simulations $N_{full.sim}$ to a more manageable number $N_{sim} \ll N_{full.sim}$. This is achieved by identifying by OAs a subset of the exhaustive factorial combinations that still captures the essential information about the input–output relationship [32,33]. An OA is a matrix where each row represents a simulation, and each column corresponds to an input random variable. The OA matrix dimensions are $(N_{sim} \times N_{IRV})$. Each element (i, j) of the OA matrix specifies a number $L_{i,j}$ (called “level”) for the j^{th} variable in the i^{th} simulation (e.g., 0 and 1 for a 2-levels OA, or 0, 1, and 2 for 3-levels OA). For example, the orthogonal array¹ $OA_4(2)^3$ for the case of three input random variables ($N_{IRV} = 3$), each one represented by two levels ($N_L = 2$), requires a minimum of four simulations

$$(N_{sim} = 4) \text{ as: } \begin{bmatrix} 000 \\ 011 \\ 101 \\ 110 \end{bmatrix}.$$

Each number $L_{i,j}$ in the OA corresponds to a sample to be assigned to

¹ An OA is represented by the symbol $OA_{N_{sim}}(N_L)^{N_{IRV}}$, using the previous definition of N_{sim} , N_L and N_{IRV} .

the j^{th} variable in the i^{th} simulation (see Subsection 2.2); in the case of three levels OA, it results in: $0 = \mu_j - \sqrt{3}/2\sigma_j$, $1 = \mu_j$ and $2 = \mu_j + \sqrt{3}/2\sigma_j$ while, for the case of two levels, it results in: $0 = \mu_j - \sigma_j$ and $1 = \mu_j + \sigma_j$. Eventually, the input matrix for the simulations in the case of three input random variables ($N_{IRV} = 3$), each one represented by two levels ($N_L = 2$)

$$\text{is: } \begin{bmatrix} \mu_1 - \sigma_1 & \mu_2 - \sigma_2 & \mu_3 - \sigma_3 \\ \mu_1 - \sigma_1 & \mu_2 + \sigma_2 & \mu_3 + \sigma_3 \\ \mu_1 + \sigma_1 & \mu_2 - \sigma_2 & \mu_3 + \sigma_3 \\ \mu_1 + \sigma_1 & \mu_2 + \sigma_2 & \mu_3 - \sigma_3 \end{bmatrix}$$

Mixed OAs, which allow for different numbers of levels per factor, can also be used. Indeed, in OABM's power system applications unmixed OAs have been usually applied and either 2 or 3 levels are assigned to all factors. Only recently, in [44] unmixed OAs have been applied in the context of a probabilistic short circuit analysis where a more detailed representation of the fault resistance is performed assigning 12 levels to this important variable. Both unmixed and mixed OAs can be constructed or found in existing repositories [45].

It should be noted that if a suitable OA of the exact size is unavailable, a larger OA can be selected and reduced by discarding redundant

obtained, the mean, standard deviations, and probability distributions can be calculated.

2.6. The optimization model

Assuming the load margin to be maximized, the following non-linear constrained optimization model including complementarity constraints can be formulated for a three-phase unbalanced power system:

$$\max \lambda \quad (1)$$

subject to

$$P_{Ri}^p - P_{Di}^p - \lambda b_{P_{Di}^p} = V_i^p \sum_{k=1}^N \sum_{m=1}^3 V_k^m [G_{ik}^{pm} \cos \theta_{ik}^{pm} + B_{ik}^{pm} \sin \theta_{ik}^{pm}] \quad (2)$$

$p = 1, 2, 3; i \in \mathcal{N}'_1$

$$Q_{Ri}^p - Q_{Di}^p - \lambda b_{Q_{Di}^p} = V_i^p \sum_{k=1}^N \sum_{m=1}^3 V_k^m [G_{ik}^{pm} \sin \theta_{ik}^{pm} - B_{ik}^{pm} \cos \theta_{ik}^{pm}] \quad (3)$$

$p = 1, 2, 3; i \in \mathcal{N}'_1$

$$P_{Gi}^T = - \sum_{p=1}^3 \sum_{m=1}^3 V_i^p V_i^m [G_{Gi}^{pm} \cos \theta_{ii}^{pm} + B_{Gi}^{pm} \sin \theta_{ii}^{pm}] + \sum_{p=1}^3 \sum_{m=1}^3 V_i^p V_j^m [G_{Gi}^{pm} \cos(\theta_{ij}^{pm}) + B_{Gi}^{pm} \sin(\theta_{ij}^{pm})] \quad (4)$$

$i, j \in \mathcal{N}'_G$

columns. The resulting array will still maintain orthogonality. Moreover, for a given number of factors and levels, OAs with different values of the so called "strength" are available. By basing the simulations on an

$$Q_{Gi}^T = - \sum_{p=1}^3 \sum_{m=1}^3 V_i^p V_i^m [G_{Gi}^{pm} \sin \theta_{ii}^{pm} - B_{Gi}^{pm} \cos \theta_{ii}^{pm}] + \sum_{p=1}^3 \sum_{m=1}^3 V_i^p V_j^m [G_{Gi}^{pm} \sin(\theta_{ij}^{pm}) - B_{Gi}^{pm} \cos(\theta_{ij}^{pm})] \quad (5)$$

$i, j \in \mathcal{N}'_G$

OA of strength t we ensure that all possible combinations of up to t of the input random variables occur together equally often [32,33]. For example, the $OA_4(2)^3$ previously shown, is an OA of strength 2; in fact, considering any two columns, each of the four possible combinations, i. e., 10, 01, 11, and 00, does appear, and they all appear the same number of times (one time, in this case). Higher-strength OAs should be suitable for systems with complex interactions or when a more detailed understanding is required. However, while increasing the number N_{sim} of simulations should improve accuracy, it typically increases computational cost.

2.4. Run deterministic VSA simulations

Once the OA and samples of the input random variables are selected, N_{sim} deterministic VSA simulations are performed to obtain the output variables of interest (i.e., maximum load margin and phase voltages). During the i^{th} run, the samples in the i^{th} row of the input matrix for the PVSA simulations are assumed as input of the N_{IRV} random variables values and the samples of the N_{ORV} output random variables are obtained by solving the nonlinear, constrained optimization model of Subsection 2.6.

2.5. Process output data

Once known the N_{sim} strings of N_{ORV} output random variables are

$$P_{Gi}^T = (P_{Gi}^T)^{sp} \quad i \in \mathcal{N}'_2 \quad (6)$$

$$V_j^1 = V_j^2 = V_j^3 \quad j \in \mathcal{N}'_{int} \quad (7)$$

$$\theta_j^1 = \theta_j^2 + 120 = \theta_j^3 - 120 \quad j \in \mathcal{N}'_{int} \quad (8)$$

$$V_s^{reg} = V_{s,0}^{reg}, \quad \theta_s^1 = 0 \quad s = \text{slack terminal bus} \quad (9)$$

$$(Q_{Gi}^T - Q_{Gi}^{min}) V_{ai} = 0 \quad i \in \mathcal{N}'_2 \quad (10)$$

$$(Q_{Gi}^T - Q_{Gi}^{max}) V_{\beta i} = 0 \quad i \in \mathcal{N}'_2 \quad (11)$$

$$V_i^{reg} = V_{i,0}^{reg} + V_{ai} - V_{\beta i} \quad i \in \mathcal{N}'_2 \quad (12)$$

$$0 \leq V_{ai} \leq V_{ai}^{max} \quad i \in \mathcal{N}'_2 \quad (13)$$

$$0 \leq V_{\beta i} \leq V_{\beta i}^{max} \quad i \in \mathcal{N}'_2 \quad (14)$$

$$Q_{Gi}^{min} \leq Q_{Gi}^T \leq Q_{Gi}^{max} \quad i \in \mathcal{N}'_2 \quad (15)$$

$$V_j^1 \leq V_j^{max} \quad j \in \mathcal{N}'_{int} \quad (16)$$

$$V_i^{p,min} \leq V_i^p \leq V_i^{p,max} \quad p = 1, 2, 3 \quad i \in \mathcal{N}_C \quad (17)$$

$$(PL_{ik}^{pp})^2 + (QL_{ik}^{pp})^2 \leq (SL_{ik}^{pp,max})^2 \quad p = 1, 2, 3 \quad ik \in \mathcal{N}_{Line} \quad (18)$$

Eqs. (2) and (3) are the active and reactive phase power balance equations at each phase of all the busbars except the internal busbars of the traditional generators (represented by the set \mathcal{N}_1); eqs. (4) and (5) are the total three-phase active and reactive power balance at each of the traditional generator terminal busbars (\mathcal{N}_G is the set containing the pairs of terminal and internal busbars of the traditional generators, including the slack one); eqs. (6) assign the total three-phase active power at all terminal nodes of the traditional generators, excluding the slack (represented by the set \mathcal{N}_2); eqs. (7) and (8) are the constraints on voltage magnitudes and arguments at the traditional generator internal busbars (represented by the set \mathcal{N}_{int}), assumed balanced; eqs. (9) are the regulation voltage equations for the slack bus and the phase angle taken as a reference; eqs. (10)-(14) are the complementary constraints (see Appendix A), at the traditional generator terminal busbars, except the slack (represented by the set \mathcal{N}_2); eqs. (15) are the limits of the total three-phase reactive power at busbars belonging to \mathcal{N}_2 ; eqs. (16) are the limits of the phase voltages at busbars belonging to \mathcal{N}_{int} ; eqs. (17) and (18) are the limits of the phase voltages at load busbars (represented by the set \mathcal{N}_C) and flows of lines (represented by the set \mathcal{N}_{Line}).

In eqs. from (1) to (18): λ is the load margin, P_{Ri}^p, Q_{Ri}^p are the active and reactive renewable powers at bus i with phase p , $P_{Di}^p, Q_{Di}^p, b_{pp}^p, b_{qp}^p$ are the active and reactive load powers in the reference conditions and the corresponding direction of increments at bus i with phase p , G_{ik}^{pm} and B_{ik}^{pm} are the real and the imaginary parts of the terms of the three-phase network admittance matrix relating bus i with phase p and bus k with phase m , V_i^p and θ_i^p are the voltage magnitude and argument at bus i with phase p , $\theta_{ik}^{pm} = \theta_i^p - \theta_k^m$, P_{Gi}^T and Q_{Gi}^T are the total three phase conventional generator active and reactive powers at bus i , G_{Gi}^{pm} and B_{Gi}^{pm} are the entries (p, m) of the 3×3 matrices $real(\bar{Y}_{Gi})$ and $imag(\bar{Y}_{Gi})$, respectively. \bar{Y}_{Gi} , the admittance matrix of the synchronous machine at bus i , is defined in [7]. V_j^{max} is the maximum limit of the internal voltage of the machine, which corresponds to the maximum field current. V_{ai} and V_{bi} are the auxiliary non-negative variables of the i^{th} generator machine, V_i^{reg} is the generator positive sequence voltage magnitude at bus i expressed as a function of the terminal generator busbar phase voltages, $V_{i,0}^{reg}$ is the assigned generator positive sequence voltage magnitude at bus i in normal conditions; PL_{ik}^{pp} and QL_{ik}^{pp} are the active and reactive powers flows in the phase p of the line connecting busses i and k expressed as functions of phase voltages and $SL_{ik}^{pp,max}$ is the maximum limit of the apparent power line flow.

It should be noted that the model of the conventional generators applied in [7] in the context of a CPF for unbalanced power systems is here applied. In this model, the three-phase terminal active power having the direction of leaving the internal bus and toward the terminal bus, and the positive-sequence voltage magnitude at terminal bus are specified. Anyway, other representations of the conventional generator busbars are possible and easily modellable; for example, the three phase total conventional generators powers cannot be assigned but limited in an interval of admissible values as well as a rate of generator power change can be introduced. Moreover, other generator voltage regulation specifications can be adopted. More details about the three-phase modelling steady-state equations can be found in [7,46].

3. Benchmark

Various methods have been proposed in the relevant literature for solving the PVSA (Probabilistic Voltage Stability Analysis), such as different Monte Carlo Simulation approaches (e.g., Traditional Monte Carlo Simulation Methods (TMCS), which use random sampling; Quasi-

Monte Carlo Simulation Methods (QMCS) and Monte Carlo Simulation Methods with Latin Hypercube Sampling (MCM-LHS), Point Estimate Methods (PEM), Cumulant-based Methods (CM), and Polynomial Chaos Expansion Methods (PCEM). For a comprehensive overview, these methods are compared and critically analyzed in several recent review papers [9,47–50], which report their characteristics and comparisons of alternative approaches and provide a summary of the pros and cons for each method.

While no universal and exhaustive considerations can be drawn about the most performing methods due to frequent strong case-dependence, the general trends are:

- (i) The accuracy of Sampling Methods (such as TMCS and QMCS) is controlled by the number of samples and generally increases (i.e., their error decreases) as the sample size grows. These methods often ensure high accuracy but require rather high computational times.
- (ii) The accuracy of Approximation Methods (such as PEM, CM, PCEM) depends on how well the underlying approximation captures the true input–output relationship, especially when strong non-linearity is present.

Given the wide range of alternatives to OABM, we selected two benchmarks to validate the proposed methodology: the Traditional Monte Carlo Simulation (TMCS) and the $2m + 1$ Point Estimate Method (PEM).

Our selection of the Traditional Monte Carlo Simulation (TMCS) and the $2m + 1$ Point Estimate Method (PEM) was deliberate. TMCS was chosen as the gold standard for uncertainty analysis due to its indisputably high accuracy, despite its known significant computational burden. Conversely, the $2m + 1$ PEM offers an attractive balance between speed and accuracy, making it a practical and frequently applied tool for uncertainty analysis in real-world power system applications.

By employing both benchmarks, we ensure that OABM is tested against both a high-fidelity, high-cost standard (TMCS) and a good-efficiency, reasonable-accuracy standard (PEM), allowing us to fully assess both its accuracy and computational efficiency.

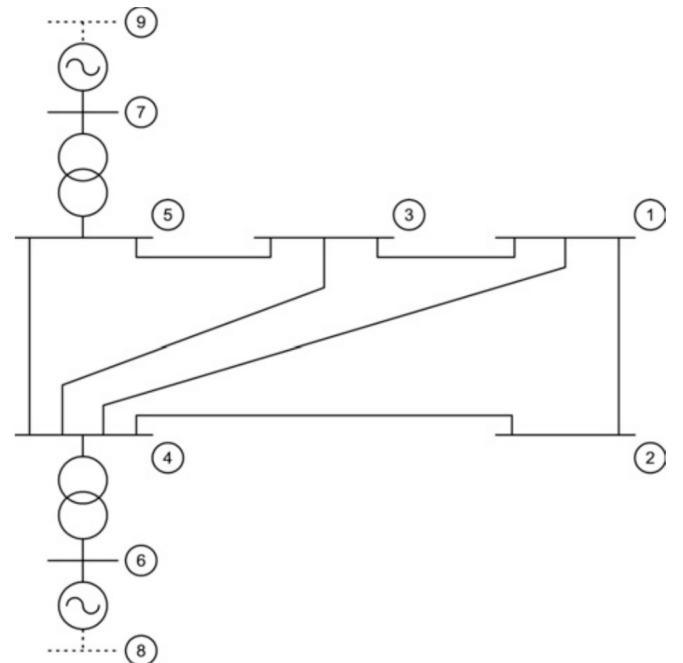


Fig. 1. Test system [12].

Table 1
Base active and reactive phase load powers.

Bus code i	Phase code p	Active power P_{Di}^p [pu]	Reactive power Q_{Di}^p [pu]
1	1	0.35	0.03
	2	0.40	0.05
	3	0.45	0.07
2	1	0.55	0.08
	2	0.60	0.10
	3	0.65	0.12
3	1	0.40	0.12
	2	0.45	0.15
	3	0.50	0.18

Specifically, in the TMCS, the vectors of correlated input random variables are generated by modeling their dependencies using a Gaussian copula. For each trial, the optimization model of Section 2.6 is solved.

The second benchmark is the $2m + 1$ Point Estimate Method (PEM), where $2m + 1$ is the total number of optimization model solutions the method requires, with m being the total number of input random variables.

The first step of the method requires calculating two representative points for each input random variable. These representative points are selected as a function of the mean values and standard deviations, and two standardized locations chosen to match some statistical moments of the input probability density functions.

The second step consists of solving $2m + 1$ times the optimization model in Section 2.6. In the first $2m$ runs, the input vectors of the model have one random variable set to one of its representative points while the remaining $m - 1$ random variables are held at their expected values. Then, an additional optimal power flow calculation is performed using only the expected values of all the input random variables; this represents the $(2m + 1)^{\text{th}}$ run.

In the third step, the moments of the output random variables are calculated using the weighting factors reported in [51].

4. Numerical applications

The OABM for PVSA of Sect. 2 has been applied to evaluate the stability limit conditions of the three-phase transmission test system shown in Fig. 1 [12] where line and load unbalances are introduced. Table 1 shows the base active and reactive loads values. The parameters are reported in [12]; only line 1–2 is unbalanced and its series-impedance and shunt-admittance matrices are reported in [12]. The bus #7 is the slack.

We chose a small grid for our analysis because, although compact, it contains all the necessary characteristics to thoroughly examine the problem addressed in this paper. Using initially a large-scale system is less advantageous, especially when the goal is precision, computational efficiency, and a clear interpretation of the results.

Indeed, a small network offers several benefits. The reduced number of nodes and lines allows to pinpoint the cause of a numerical issue, like an overloaded line or an abnormal voltage. This simplifies debugging

Table 2
Generator positive sequence voltage magnitude and three-phase active power in the base operating point.

$V_{6,0}^{\text{reg}}$ [pu]	1.045
$V_{\text{slack},0}^{\text{reg}}$ [pu]	1.06
$(P_{G6}^T)^{\text{sp}}$ [pu]	1.2

Table 3
Lower and upper bounds of generator three-phase reactive power.

Bus code i	Three-phase reactive power [pu]	
	min	max
6	-1.2	1.5

and model validation. A smaller system also allows for a deeper understanding of its behaviour, as cause-and-effect relationships are more direct and less obscured by complex side effects.

The positive sequence voltage magnitude $V_{6,0}^{\text{reg}}$ and $V_{\text{slack},0}^{\text{reg}}$ at generator busbars #6 and #7 and the three-phase active power $(P_{G6}^T)^{\text{sp}}$ at generator busbar #6 (base operating point) are reported in Table 2 while the lower and upper bounds for generator three-phase reactive powers are in Table 3. The phase voltage magnitude is constrained between 0.8 and 1.1. p.u. for busbars from #1 to #5.

With reference to the input random variables, the test system in Fig. 1 includes 2 wind plants at bus #1 and bus #2 whose characteristics are reported in [52]. The wind speeds are correlated with the correlation coefficient being 0.85 and following the Weibull distribution $W(11.2, 3.81)$. The direction of increments of both active and reactive loads powers are described by uncorrelated normal distributions in Case A and by correlated normal distributions in Case B; the mean values are the base loads (Table 1) and the standard deviations are 10 % of the mean [12,14]. In Case B the direction of increments of active and reactive loads powers are correlated with the correlation coefficient being 0.80. For the application of the Point Estimate Method, the correlation among input random variables was handled using the procedure proposed in [53]. For the application of OABM, the heuristic procedure considered in [39,54] was applied, which effectively includes correlated variables in both optimization problems [54] and load flow calculations [39] for different networks. The reasons why this procedure, even though heuristic, seemed reasonable are that it firstly transforms the correlated variables into uncorrelated variables to apply the Orthogonal Array not in the original complex space, but in the uncorrelated space. Then, an inverse transformation maps the points back to the configuration required for the simulation of the physical system which operates only with the correlated variables.

The algorithm applied to solve the optimization problem is based on the sequential quadratic programming method available in MATLAB® optimization toolbox. Numerical applications were executed on a system equipped with an Intel Core i7-12700 CPU running at 2.10 GHz (12th generation) and 32 GB of RAM.

The PVSA was performed with the application of OABM by solving the optimization problem formulated in Section 2.6. The probabilistic characterization of the optimal value of the load margin λ and of the voltage magnitudes and arguments at the three phases of each bus were then determined.

Several cases of OAs, in terms of the chosen array size and its strength, were considered [45]:

- i) Orthogonal array with 2 levels, strength 2, with $N_{\text{sim}} = 32$, referred to as $OA_{32}(2)^{N_{\text{IRV}}}$;
- ii) Orthogonal array with 2 levels, strength 3, with $N_{\text{sim}} = 40$, referred to as $OA_{40}(2)^{N_{\text{IRV}}}$;
- iii) Orthogonal array with 3 levels, strength 2, with $N_{\text{sim}} = 81$, referred to as $OA_{81}(3)^{N_{\text{IRV}}}$;
- iv) Orthogonal array with 3 levels, strength 3, with $N_{\text{sim}} = 243$, referred to as $OA_{243}(3)^{N_{\text{IRV}}}$,

being $N_{\text{IRV}} = 20$.

As our reference method, we employed the traditional Monte Carlo Simulation (MCS) approach, conducting 200,000 trials. To provide a

Table 4

Percentage errors for OABM PVSA with 2 levels-orthogonal arrays and for PEM (%) – Case A.

	Phase voltage magnitude		Phase voltage argument		Load margin	
	Mean value (%)	Standard deviation (%)	Mean value (%)	Standard deviation (%)	Mean value (%)	Standard deviation (%)
$OA_{32}(2)^{N_{IRV}}$	0.0111	8.5986	0.0171	5.1279	0.0695	3.5406
$OA_{40}(2)^{N_{IRV}}$	0.0070	2.1041	0.0103	1.4948	0.0615	1.6537
PEM	0.0696	19.6147	0.1040	8.9683	0.4687	2.4481

comparison with another probabilistic approximation method, we applied the Point Estimate Method (PEM) with $2n + 1$ points. Here, $2n + 1$ represents the total number of optimization model solutions required by the method, where n is the total number of input random variables, i. e., 41, given that $n = N_{IRV} = 20$. The traditional MCS was chosen as the reference due to its indisputably high accuracy. In turn, the $2n + 1$ PEM was applied because it offers a good balance between accuracy and computational burden, making it a practical and valuable tool for incorporating uncertainty analysis into various power system applications.

Case A

First, an analysis of accuracy of the results obtained by applying the OABM for PVSA is reported. For each OA considered, the *percentage errors* of the statistical metrics of the load margin, the magnitudes and arguments of the phase voltages are determined assuming the results of MCS as reference values. As statistical metrics, the mean value and the standard deviation are considered. Since the voltage magnitudes and arguments concern all the system busbars, the average values of their errors (over the busbars) are calculated.

Table 4 report the average percentage errors of the statistical features relative to the phase voltage magnitudes and arguments, and the load margin for the two-levels OA $OA_{32}(2)^{N_{IRV}}$, strength 2, the two-levels OA $OA_{40}(2)^{N_{IRV}}$, strength 3, and for $2n + 1$ PEM. We can observe that:

- the errors of $OA_{40}(2)^{N_{IRV}}$ are lower than those of $OA_{32}(2)^{N_{IRV}}$.
- Comparing the results of case $OA_{32}(2)^{N_{IRV}}$ with the ones of PEM, it arises that the OABM exhibits errors lower than the corresponding ones of the PEM procedure, except for the standard deviation of load margin; in some cases, the errors are significantly lower, in other case, they are of the same order of magnitude.
- Comparing the results of case $OA_{40}(2)^{N_{IRV}}$ with the ones of PEM, it arises that the OABM exhibits always errors significantly lower than the corresponding ones of the PEM procedure.

Eventually, given that we are comparing three cases with a similar number of simulations (specifically, 32 or 40 for OABM and 41 for PEM), our analysis indicates that OABM outperforms PEM. This is evident in its superior accuracy as strength increases, even when the computational effort (represented by the number of simulations) is comparable.

While the aim of the first analysis was to establish a comparison among procedures with similar computational burden, we perform now further analysis considering the solution of the OABM with three-levels OAs, requiring a greater number of simulations than PEM (i.e., 81 or 243 for OABM versus 41 for PEM) and then greater computational efforts.

Table 5

Percentage errors for OABM PVSA with 3 levels-orthogonal arrays and for PEM (%) – Case A.

	Phase voltage magnitude		Phase voltage argument		Load margin	
	Mean value	Standard deviation	Mean value	Standard deviation	Mean value	Standard deviation
$OA_{81}(3)^{N_{IRV}}$	0.0113	5.1019	0.0163	0.5877	0.0906	0.1514
$OA_{243}(3)^{N_{IRV}}$	0.0037	1.4296	0.0037	0.7859	0.0227	0.0513
PEM	0.0696	19.6147	0.1040	8.9683	0.4687	2.4481

Table 5 report the average percentage errors of the statistical features relative to the phase voltage magnitudes and arguments, and load margin for the three-levels OA $OA_{81}(3)^{N_{IRV}}$, strength 2, the three-levels OA array $OA_{243}(3)^{N_{IRV}}$, strength 3, and once again $2n + 1$ PEM.

Based on the results reported in Table 5, we can observe that the errors of $OA_{243}(3)^{N_{IRV}}$ are lower than those of $OA_{81}(3)^{N_{IRV}}$, with the exception of the standard deviation of voltage arguments, which exhibits a similar value. Once again, increasing strength proves more effective.

Regarding the accuracy, the three-levels OABM always significantly outperforms the PEM with the case with $N_{sim} = 243$ yielding the most accurate results despite the highest computational efforts. Indeed, the case $OA_{81}(3)^{N_{IRV}}$ offers a good compromise between the accuracy of results and computational burden. For this last case, as a further example of obtained results, the mean values and standard deviations of the variables of interest are reported in Tables 6-7, compared to the MCS values.

Moreover, Figs. 2-3 show the cumulative distribution functions (CDFs) of the load margin and of the phase voltage magnitudes at busbar #4 obtained with the traditional MCS, OABM for case $OA_{81}(3)^{N_{IRV}}$ and PEM. The CDFs obtained with OABM and with PEM are close to the CDFs obtained with the 200,000 samples of MCS.

Eventually, in Tables 8-9, the minimum, the mean and the maximum percentage errors of percentiles of load margin and of phase voltage magnitudes (node #4) with respect to the traditional MCS are reported for the case $OA_{81}(3)^{N_{IRV}}$ and for PEM. Except for a few cases, the OABM with $OA_{81}(3)^{N_{IRV}}$ obtains better results also in terms of percentiles errors.

Case B

To assess the accuracy of the results obtained by applying the OABM for PVSA, the average percentage errors of the statistical features relative to the phase voltage magnitudes and arguments, and the load margin with respect to MCS for the two-levels OA $OA_{32}(2)^{N_{IRV}}$, strength 2, the two-levels OA $OA_{40}(2)^{N_{IRV}}$, strength 3, and for PEM are reported in Table 10. We can observe that:

- the errors of $OA_{40}(2)^{N_{IRV}}$ are lower than those of $OA_{32}(2)^{N_{IRV}}$ except for the errors of the standard deviation of the load margin and of the mean value of the phase voltage arguments (0.0011 versus 0.0010 %).
- Comparing the results of case $OA_{32}(2)^{N_{IRV}}$ (strength 2) with the ones of PEM, it arises that the OABM exhibits errors smaller than the corresponding ones of the PEM procedure, except for the standard deviation of phase voltage magnitudes and arguments and for the mean value of the load margin (even if with very small differences).

Table 6

Mean value of the phase voltage magnitudes at load busbars at critical point for OABM with $OA_{81}(3)^{N_{RV}}$ and for MCS (p.u.) – Case A.

Load bus	Phase 1				Phase 2				Phase 3			
	Mean value	Mean value	Standard deviation	Standard deviation	Mean value	Mean value	Standard deviation	Standard deviation	Mean value	Mean value	Standard deviation	Standard deviation
	OABM	MCS	OABM	MCS	OABM	MCS	OABM	MCS	OABM	MCS	OABM	MCS
#1	1.0367	1.0366	0.0094	0.0095	1.0333	1.0332	0.0138	0.0139	0.8026	0.8028	0.0061	0.0072
#2	1.0356	1.0355	0.0096	0.0097	1.0342	1.0341	0.0138	0.0139	0.8019	0.8021	0.0061	0.0072
#3	1.0349	1.0348	0.0092	0.0093	1.0334	1.0333	0.0135	0.0136	0.8071	0.8074	0.0064	0.0075
#4	1.0351	1.0351	0.0061	0.0061	1.0708	1.0707	0.0086	0.0088	0.9085	0.9087	0.0051	0.0058
#5	1.0520	1.0519	0.0054	0.0054	1.0910	1.0909	0.0072	0.0074	0.9479	0.9480	0.0047	0.0052

Table 7

Mean value and standard deviation of the load margin for OABM PVSA with $OA_{81}(3)^{N_{RV}}$ and for MCS (p.u.) – Case A.

	Mean value		Standard deviation	
	OABM	MCS	OABM	MCS
Load margin	0.8202	0.8194	0.1059	0.1061

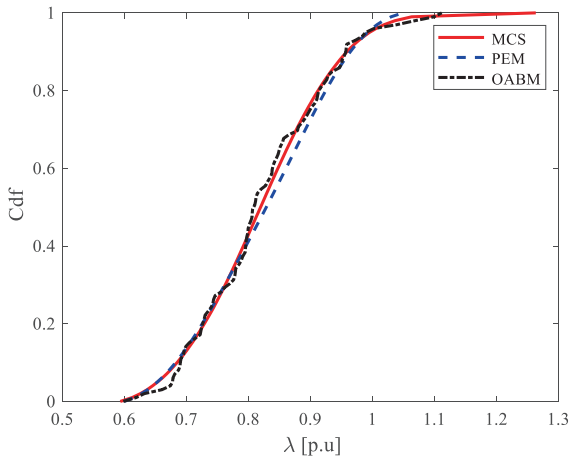


Fig. 2. CDFs of the load margin obtained with the traditional MCS (200,000 trials), with OABM for case $OA_{81}(3)^{N_{RV}}$ and with PEM – Case A.

- Comparing the results of case $OA_{40}(2)^{N_{RV}}$ (strength 3) with the ones of PEM, it arises that the OABM exhibits errors lower than the corresponding ones of the PEM procedure except for the standard deviation of the phase voltage arguments and of the load margin (even if with very small differences).

The OABM accuracy with strength 3 is also better in Case B, though to a lesser degree compared to Case A, even with a similar number of simulations. The OABM accuracy with strength 2 is similar to the one of PEM.

When three-levels OAs are chosen, using a number of simulations greater than PEM (i.e., 81, 243 for OABM versus 41 for PEM), the results of percentage errors with respect to MCS are reported in Table 11. We can observe that the errors of $OA_{243}(3)^{N_{RV}}$ are lower than those of $OA_{81}(3)^{N_{RV}}$, with the exception of the load margin (mean value and standard deviation) and PEM exhibits errors greater than the ones obtained with the OABM.

Also in this case, the OABM PVSA with $OA_{81}(3)^{N_{RV}}$ is chosen to show more results. In particular, in Table 12, the mean value and the standard deviation of the load margin obtained with OABM are compared with the ones obtained with the MCS. Figs. 4 and 5 show the CDFs of the load

Table 8

Minimum, mean, maximum percentage errors of percentiles of load margin with respect to traditional MCS (%) – Case A.

	Minimum	Mean	Maximum
$OA_{81}(3)^{N_{RV}}$	0.0178	1.0375	12.0005
PEM	0.0190	1.0133	16.9515

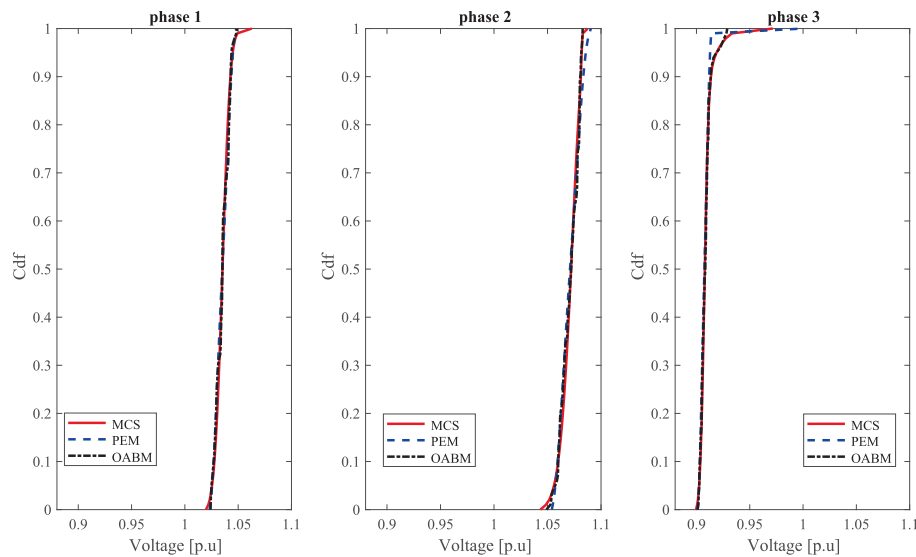


Fig. 3. CDFs of the voltage magnitudes at phase 1, phase 2 and phase 3 of busbar #4, obtained with the traditional MCS (200,000 trials), with OABM for case $OA_{81}(3)^{N_{RV}}$ and with PEM – Case A.

Table 9

Minimum, mean, maximum percentage errors of percentiles of phase voltage magnitudes (node #4) with respect to MCS (%) – Case A.

	Phase 1			Phase 2			Phase 3		
	Minimum	Mean	Maximum	Minimum	Mean	Maximum	Minimum	Mean	Maximum
$OA_{81}(3)^{N_{RV}}$	0.0012	0.0896	1.3059	0.0006	0.0969	0.5425	0.0007	0.0848	4.3934
PEM	0.0014	0.0921	1.3732	0.0013	0.1621	1.0272	0.0015	0.1517	2.9245

Table 10

Percentage errors for OABM with 2 levels-orthogonal arrays and for PEM (%) – Case B.

	Phase voltage magnitude		Phase voltage argument		Load margin	
	Mean value (%)	Standard deviation (%)	Mean value (%)	Standard deviation (%)	Mean value (%)	Standard deviation (%)
$OA_{32}(2)^{N_{RV}}$	0.0017	8.5949	0.0010	1.8432	0.0487	0.1871
$OA_{40}(2)^{N_{RV}}$	0.0008	6.9816	0.0011	1.0223	0.0002	0.9063
PEM	0.0026	7.9449	0.0032	0.7455	0.0138	0.5782

Table 11

Percentage errors for OABM with 3 levels-orthogonal arrays and for PEM (%) – Case B.

	Phase voltage magnitude		Phase voltage argument		Load margin	
	Mean value	Standard deviation	Mean value	Standard deviation	Mean value	Standard deviation
$OA_{81}(3)^{N_{RV}}$	0.0012	6.8096	0.0016	0.3181	0.0022	0.1307
$OA_{243}(3)^{N_{RV}}$	0.0002	1.1664	0.0002	0.1577	0.0077	0.3439
PEM	0.0026	7.9449	0.0032	0.7455	0.0138	0.5782

Table 12

Mean value and standard deviation of the load margin for OABM with $OA_{81}(3)^{N_{RV}}$ and for MCS (p.u.) – Case B.

	Mean value		Standard deviation	
	$OA_{81}(3)^{N_{RV}}$	MCS	$OA_{81}(3)^{N_{RV}}$	MCS
Load margin	0.8264	0.8265	0.1193	0.1195

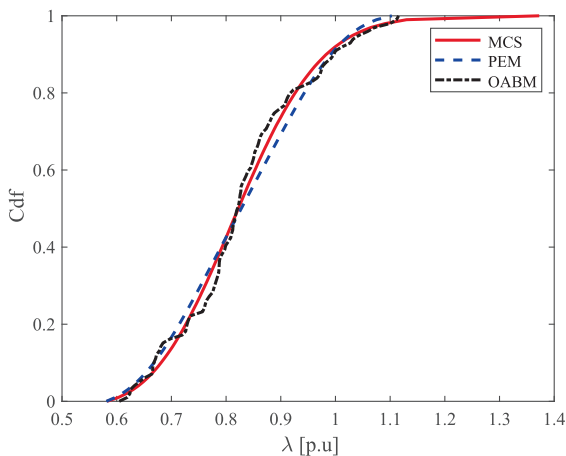


Fig. 4. Cdf of the load margin obtained with the classical MCS (200,000 trials), with OABM for case $OA_{81}(3)^{N_{RV}}$ and with PEM – Case B.

margin and of the phase voltage magnitudes at busbar #4 obtained with OABM, PEM and MCS; also in this case the CDF are close each other. The errors of percentiles were calculated and considerations similar to Case A were drawn.

Finally, the applied methods are compared based on the computational time. Assuming that the number of simulations to be solved is closely linked to the overall computational burden and can be used as an

approximate measure of computational effort, from the analysis of the total number of simulations required by the traditional Monte Carlo method (200.000 runs of optimization), the $2m + 1$ PEM (41 runs of optimization), and the OABM (runs ranging in the interval 32–243 depending on the selected OA) it's clear that the proposed method employing the OA array with 2 levels and strength 2 should be the least burdensome and the Monte Carlo method should be the most burdensome.

5. Conclusions

Probabilistic voltage stability analysis requires careful consideration of uncertainties of input random variables and often necessitates substantial computational efforts. To address these challenges, this paper has proposed an approach based on the Orthogonal Arrays. The approach aims to mitigate computational efforts while ensuring high results accuracy. OAs of different strengths have been applied and numerical applications to a test system have been performed comparing the output results of the proposed approach with the ones of more traditional probabilistic approaches.

The main outcomes of the paper are that in the examined cases:

- The OABM accurately models uncertainties of PVSA input random variables, confirming its effectiveness in solving power systems problems.
- The two and three-levels OA ensure high accuracy while significantly reduced computational costs compared to traditional Monte Carlo simulation procedures.
- Higher strength OAs have shown better performances, albeit with increased computational demands compared to lower strengths.
- The two-levels OA has demonstrated similar or even better accuracy and comparable computational efforts with respect to a $2n + 1$ PEM approach, while the three-level OABM has shown overall better accuracy, albeit with increased computational demands compared to the $2n + 1$ PEM approach.

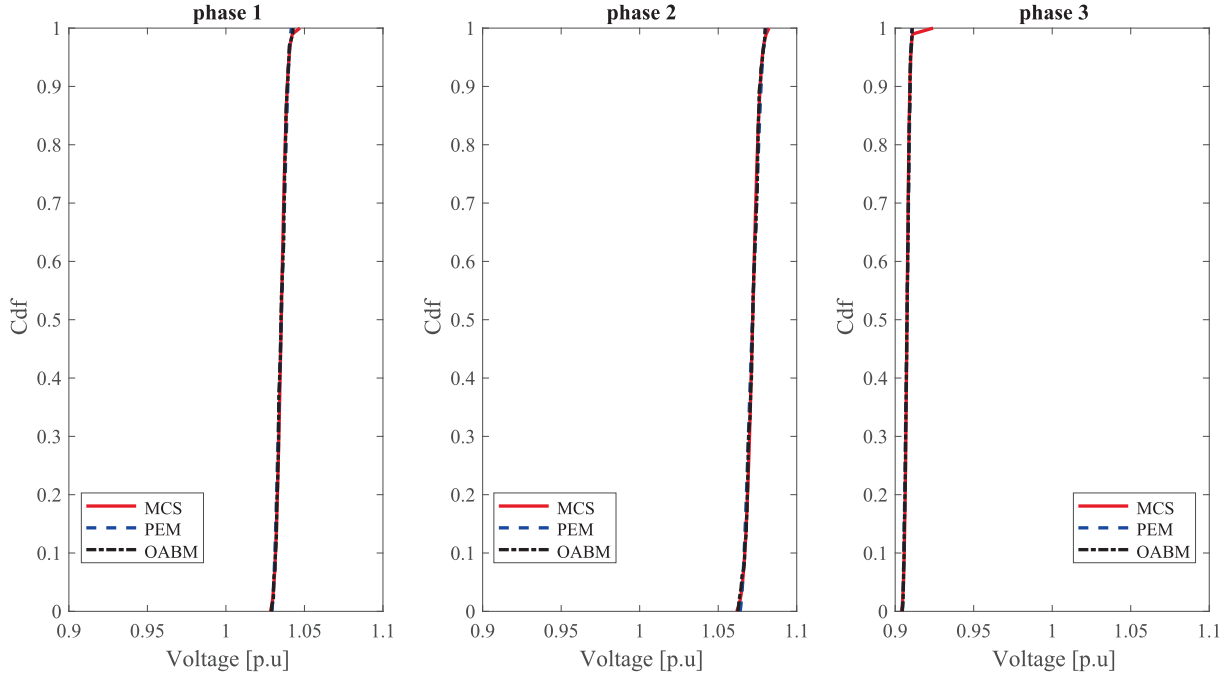


Fig. 5. Cdfs of the voltage magnitudes at phase 1, phase 2 and phase 3 of busbar #4, obtained with the classical MCS (200,000 trials), with OABM for case $OA_{81}(3)^{N_{rv}}$ and with PEM – Case B.

Advanced Orthogonal Arrays techniques are currently under investigation to further reduce computational costs and increase result accuracy. Moreover, further tests of the proposed approach on high-dimension models will be the subject of a future paper where new and advanced tools for handling the correlations and advanced algorithms will be tested.

CRedit authorship contribution statement

Guido Carpinelli: Writing – review & editing, Writing – original draft, Validation, Supervision, Methodology, Investigation, Conceptualization. **Angela Russo:** Writing – review & editing, Writing – original

draft, Validation, Supervision, Software, Methodology, Investigation, Conceptualization. **Pietro Varilone:** Writing – review & editing, Writing – original draft, Validation, Supervision, Software, Methodology, Investigation, Conceptualization. **Paola Verde:** Writing – review & editing, Writing – original draft, Validation, Supervision, Methodology, Investigation, Conceptualization.

Declaration of competing interest

The authors declare that they have no known competing financial interests or personal relationships that could have appeared to influence the work reported in this paper.

Appendix A

In different categories of problems, CCs are very useful in modelling a change in system behaviour [55–57]; in particular, CCs have been successfully used in VS optimization problems for modelling traditional generators (based on synchronous generator) switch from a PV bus to a PQ bus as the reactive power limit of the generators is reached [5,55]. A three-phase model of traditional generators via CCs was also formulated in [12]. It is recognized that the CCs, being non-convex and non-smooth, can lead to convergence problems and to multiple solutions of the non-linear optimization problems; however, due to the advances in nonlinear programming solvers and thanks to specific approaches to avoid numerical issues (e.g., the ones reported in [56]), feasible, at least local optimal solution is guaranteed.

The change from a PV to a PQ busbar in an unbalanced three phase power system can be modelled by the following equality constraints:

$$(Q_{Gi}^T - Q_{Gi}^{min})V_{\alpha i} = 0 \quad (A.1)$$

$$(Q_{Gi}^T - Q_{Gi}^{max})V_{\beta i} = 0$$

$$V_i^{reg} = V_{i,0}^{reg} + V_{\alpha i} - V_{\beta i}$$

where $V_{\alpha i}$ and $V_{\beta i}$ are auxiliary non-negative variables that allow increasing or decreasing the generator positive sequence voltage magnitude V_i^{reg} respect to the value $V_{i,0}^{reg}$ in normal condition, depending on the value of Q_{Gi}^T , i.e. is the three-phase reactive power; in (A.1) Q_{Gi}^{min} and Q_{Gi}^{max} are the lower

and upper permissible values for Q_{Gi}^T .

From the analysis of (A.1) the generator operating modes are as follows:

$$\text{if } Q_{Gi}^T = Q_{Gi}^{\min} \rightarrow V_{ai} \geq 0 \text{ and } V_{\beta i} = 0 \rightarrow V_i^{\text{reg}} = V_{i,0}^{\text{reg}} + V_{ai} \quad (\text{A.2})$$

$$\text{if } Q_{Gi}^T = Q_{Gi}^{\max} \rightarrow V_{ai} = 0 \text{ and } V_{\beta i} \geq 0 \rightarrow V_i^{\text{reg}} = V_{i,0}^{\text{reg}} - V_{\beta i}$$

$$\text{if } Q_{Gi}^{\min} < Q_{Gi}^T < Q_{Gi}^{\max} \rightarrow V_{ai} = 0 \text{ and } V_{\beta i} = 0 \rightarrow V_i^{\text{reg}} = V_{i,0}^{\text{reg}}$$

Data availability

No data was used for the research described in the article.

References

- [1] P. Kundur et al., Definition and classification of power system stability. IEEE/CIGRE joint task force on stability terms and definitions. IEEE Trans Power Syst. 2004;19(3):1387–1401.
- [2] Gomez Esposito A, Conejo AJ, Canizares C. Electric Energy Systems Analysis and operation. New York: Taylor & Francis Group; 2009.
- [3] Kundur P. Power System Stability and Control. New York, USA: McGraw Hill; 1994.
- [4] Van Cutsem T. Voltage instability: phenomena, countermeasures, and analysis methods. Proc IEEE 2000;88(2):208–27.
- [5] Avalos RJ, Canizares CA, Milano F, Conejo AJ. Equivalency of continuation and optimization methods to determine saddle-node and limit-induced bifurcations in power systems. IEEE Trans Circuits Syst 2009;56(1):210–22.
- [6] Sode-Yome A, Mithulananthan N, Lee K. A maximum loading margin method for static voltage stability in power systems. IEEE Trans on Power Syst 2006;21(2):799–808.
- [7] Zhang XP, Ju P, Handschin E. Continuation three-phase power flow: a tool for voltage stability analysis of unbalanced three-phase power systems. IEEE Trans Power Syst 2005;21(3):1320–9.
- [8] Carpinelli G, Lauria D, Varilone P. Voltage stability analysis in unbalanced power systems by optimal power flow. IEE Proc Gen, Trans, Distrib 2006;153(3):261–8.
- [9] Aien M, Hajebrahimi A, Fotuhi-Firuzabad M. A comprehensive review on uncertainty modeling techniques in power system studies. Renew Sustain Energy Rev 2016;57:1077–89.
- [10] Liu Ky, Sheng W, Hu L, Liu Y, Meng X, Jia D. Simplified probabilistic voltage stability evaluation considering variable renewable distributed generation in distribution systems. IET Gener Transm Distrib 2015;9:1464–1473.
- [11] Ran X, Miao S. Probabilistic evaluation for static voltage stability for unbalanced three-phase distribution system. IET Gener Transm Distrib 2015;9:2050–9.
- [12] Carpinelli G, Caramia P, Russo A, Varilone P. Voltage stability in unbalanced power systems: a new complementarity constraints-based approach. IET Gener, Transm & Distrib 2015;9(14):2014–202.
- [13] Deng W, Zhang B, Ding H, Li H. Risk-based probabilistic voltage stability assessment in uncertain power system. Energies 2017;10(180):1–19.
- [14] Xu X, Yan Z, Shahidepour M, Wang H, Chen S. Power system voltage stability evaluation considering renewable energy with correlated variabilities. IEEE Trans Power Syst 2018;33(3):3236–45.
- [15] Tourandaz Kenari M, Sepasian MS, Setayesh Nazar M. Probabilistic voltage stability assessment of distribution networks with wind generation using combined cumulants and maximum entropy method. Int J Electr Power Energy Syst 2018;95:96–107.
- [16] Tourandaz Kenari M, Sepasian MS, Setayesh Nazar M. Probabilistic assessment of static voltage stability in distribution systems considering wind generation using catastrophe theory. IET Gener Transm Distrib 2019;13:2856–65.
- [17] Zhao J, Bao Y, Chen G. Probabilistic voltage stability assessment considering stochastic load growth direction and renewable energy generation. In: 2018 IEEE Power & Energy Society General Meeting (PESGM), Portland, OR, USA; 2018. p. 1–5.
- [18] Qi B, Hasan KN, Milanović JV. Identification of critical parameters affecting voltage and angular stability considering load-renewable generation correlations. IEEE Trans on Power Syst 2019;34(4):2859–69.
- [19] Zhang J, et al. A probabilistic assessment method for voltage stability considering large scale correlated stochastic variables. IEEE Access 2020;8:5407–15.
- [20] Xia C, Zheng X, Guan L, Baig S. Probability analysis of steady-state voltage stability considering correlated stochastic variables. Int J Electr Power Energy Syst 2021;131:107105.
- [21] Rahman S, Saha S, Haque ME, Islam SN, Arif MT, Mosadeghy M, et al. A framework to assess voltage stability of power grids with high penetration of solar PV systems. Int J Electr Power Energy Syst 2022;139:107815.
- [22] Rahman MT, Hasan KN, Sokolowski P. Evaluation of wind farm aggregation using probabilistic clustering algorithms for power system stability assessment. Sustain Energy, Grids Netw 2022;30:1–10.
- [23] Wang C, Wang L, Deng X, Liu J, Guo D. Scenario-based line switching for enhancing static voltage stability with uncertainty of renewables and loads. Int J Electr Power Energy Syst 2023;145:108653.
- [24] Guo D, Wang L, Jiao T, Wu K, Yang W. Day-ahead voltage-stability-constrained network topology optimization with uncertainties. J Mod Power Syst Clean Energy 2024;12(3):730–41.
- [25] Wang Q, Lin S, Yang Y, Liu W, Yang Z, Ye J, et al. Distributed bi-level optimal power flow calculation for SVSM interval of integrated transmission and distribution networks considering the uncertain renewables. Int J Electr Power Energy Syst 2023;152:109276.
- [26] Peng S, Lin X, Tang J, Xie K, Ponci F, Monti A. A set of novel global sensitivity analysis indices for probabilistic static voltage stability assessment with correlated uncertainty sources. IEEE Trans on Power Syst 2024;39(2):2543–57.
- [27] Alzubaidi M, Hasan KN, Meegahapola L. Probabilistic steady-state and short-term voltage stability assessment considering correlated system uncertainties. Electr Pow Syst Res 2024;228:110008.
- [28] Su H-Y, Hong H-H. An Intelligent data-driven learning approach to enhance online probabilistic voltage stability margin prediction. IEEE Trans on Power Syst 2021;36(4):3790–3.
- [29] Su H-Y, Lai C-C. Dynamic-deep-ensemble-learning scheme for probabilistic voltage stability margin estimation to enhance resilient power grid monitoring. IEEE Trans Ind Appl 2024;60(2):2065–2075.
- [30] Yang H, Shi X, Qiu RC, He X, Ai Q, Wang Z. Monitoring data factorization of high renewable energy penetrated grids for probabilistic static voltage stability assessment. IEEE Trans on Smart Grid 2022;13(2):1273–86.
- [31] Nejadfard-jahromi S, Mohammadi M. Data-driven look-ahead voltage stability assessment of power system with correlated variables. IET Gener Transm Distrib 2022;16:1795–807.
- [32] Roy RK. Design of experiments using the Taguchi approach. New York: John Wiley & Sons; 2001.
- [33] Hedayat AS, Sloane NJA, Stufken J. Orthogonal arrays: theory and applications. New York: Springer Series in Statistics; 1999.
- [34] Liu D, Cai Y. Taguchi method for solving the economic dispatch problem with nonsmooth cost functions. IEEE Trans Power Syst 2005;20(4):2006–14.
- [35] Yu H, Chung CY, Wong KP. Robust transmission network expansion planning method with Taguchi's orthogonal array testing. IEEE Trans Power Syst 2011;26(3):1573–80.
- [36] Yu H, Rosehart WD. An optimal power flow algorithm to achieve robust operation considering load and renewable generation uncertainties. IEEE Trans Power Syst 2012;27(4):1808–17.
- [37] Basetti V, Chandel AK. Hybrid power system state estimation using Taguchi differential evolution algorithm. IET Sci Meas Technol 2015;9(4):449–66.
- [38] Hong YY, Lin FJ, Yu TH. Taguchi method-based probabilistic load flow studies considering uncertain renewables and loads. IET Renew Power Gener 2016;10:221–7.
- [39] Carpinelli G, Rizzo R, Caramia P, Varilone P. Taguchi's method for probabilistic three-phase power flow of unbalanced distribution systems with correlated wind and photovoltaic generation systems. Renew Energy 2018;117:227–41.
- [40] Meena NK, et al. Modified Taguchi-based approach for optimal distributed generation mix in distribution networks. IEEE Access 2019;7:35689–702.
- [41] Hong YY, Nguyen N. Multiobjective multicriteria under-frequency load shedding in a standalone power system. IEEE Syst J 2020;14:2759–69.
- [42] Reza Nikzad H, Abdi H. A robust unit commitment based on GA-PL strategy by applying TOAT and considering emission costs and energy storage systems. Electr Power Syst Res 2020;180:106154.
- [43] Carpinelli G, Russo A, Varilone P, Verde P. Polynomial normal transformations and quasi monte carlo method for probabilistic voltage stability analysis. Int Trans Electr Energy Syst.
- [44] Bracale A, Caramia P, Carpinelli G, De Falco P, Verde P. A mixed Taguchi-based probabilistic short circuit analysis for unbalanced distribution systems with PV systems in low-voltage ride-through. J Mod Power Syst Clean Energy 2025;13(5):1738–51.
- [45] Sloane NJA. A library of orthogonal arrays. Available online: <http://neilsloane.com/oadir/>.
- [46] Arrillaga J, Harnold CP, Harker BJ. Computer analysis of power systems. J Wiley, USA; 1990.
- [47] Nazmul Hasan K, Preece R, Milanović JV. Existing approaches and trends in uncertainty modelling and probabilistic stability analysis of power systems with renewable generation. Renew Sustain Energy Rev 2019;101:168–80.

- [48] Wanjoli P, Abbasy NH, Zakaria Moustafa MM. A state-of-the-art review on the modeling and probabilistic approaches to analysis of power systems integrated with distributed energy resources. *Ain Shams Eng J* 2025;16(1):103198.
- [49] Hakami AM, Hasan KN, Alzubaidi M, Datta M. A review of uncertainty modelling techniques for probabilistic stability analysis of renewable-rich power systems. *Energies* 2023;16.
- [50] Ebeed M, Abdel Aleem SHE. Chapter 1 - Overview of uncertainties in modern power systems: uncertainty models and methods. In: *Uncertainties in Modern Power Systems*, eds. A. F. Zobaa, S. H.E. Abdel Aleem, Academic Press, 2021.
- [51] Bautista LGC, Soares J, Baquero JFF, Vale Z. Probabilistic algorithm based on 2m+1 point estimate method edgeworth considering voltage confidence intervals for optimal PV generation. In: *17th Int. Conf. on Probabilistic Methods Applied to Power Systems (PMAPS)*, June 2022. pp. 1–6.
- [52] Yang H, Zou B. The point estimate method using third-order polynomial normal transformations technique to solve probabilistic power flow with correlated wind source and loads. In: *Proc of Asia-Pacific Power and Energy Eng. Conf.*, 27-29 March 2012, Shanghai, China.
- [53] Morales JM, Baringo L, Conejo AJ, Mínguez R. Probabilistic power flow with correlated wind sources. *IET Gener Transm & Distrib* 2010;4:641–51.
- [54] Najjarpour M, Tousei B, Jamali S. Loss reduction in distribution networks with DG units by correlating taguchi method and genetic algorithm. *Iran J Electr Electron Eng* 2022;18.
- [55] Rosehart W, Roman C, Schellenberg A. Optimal power flow with complementarity constraints. *IEEE Trans on Power Syst* 2005;20(2):813–22.
- [56] Capitanescu F, Rosehart W, Wehenkel L. Optimal power flow computations with constraints limiting the number of control actions. *IEEE PowerTech Conf., Bucharest (Romania)*; 2009.
- [57] Capitanescu F. Can we compute the worst voltage case under power flows uncertainty at TSO-DSO interfaces? *Electr Pow Syst Res* 2024;234:110613.